

Average intensity of flattened Gaussian beam in non-Kolmogorov turbulence

Xiuxiang Chu^{b,*}, Chunhong Qiao^a, Xiaoxing Feng^a

^a Key Laboratory of Atmospheric Composition and Optical Radiation, Chinese Academy of Sciences, Hefei 230031, China

^b School of sciences, Zhejiang Agriculture and Forestry University, Lin'an 311300, China

ARTICLE INFO

Article history:

Received 11 November 2010

Received in revised form

19 February 2011

Accepted 2 March 2011

Available online 21 March 2011

Keywords:

Flattened Gaussian beam

Non-Kolmogorov turbulent atmosphere

Propagation

ABSTRACT

Based on the extended Huygens–Fresnel principle and the first-order approximation of wave structure function, an analytical expression for the average intensity of flattened Gaussian beam (FGB) in non-Kolmogorov turbulence has been derived. The variations of normalized intensity with some parameters, such as wave coherence length, Fresnel number, waist width and the order of FGB are investigated in detail.

© 2011 Elsevier Ltd. All rights reserved.

1. Introduction

The classical Kolmogorov turbulence has played a most important role in the development of atmospheric and adaptive optics. It has shown good agreement with many experiments. However, there also exist some experimental data that deviated from Kolmogorov theory [1–4]. Namely, they may exhibit non-Kolmogorov turbulence in atmosphere. During past decades, much attention has been given to the propagation and compensation of beams in non-Kolmogorov turbulence. Many investigations into the properties of beam in non-Kolmogorov turbulence have been reported [5–14].

To improve system performance, the propagations of various types of laser beams in Kolmogorov turbulence have been widely studied [15–21]. However, to the best of our knowledge, the properties of many types of beams in non-Kolmogorov turbulence have not been taken into account. In our present work, the average intensity of flattened Gaussian beam in non-Kolmogorov turbulence is studied. Our motivation is to investigate the properties of FGB with different power spectrum of refractive index fluctuations. It is noteworthy that the outer and inner scales of turbulence will impact on the average intensity. For the sake of simplicity, the analysis in the present paper is restricted to the inertial interval of turbulence spectrum. The effects due to outer and inner scales are neglected.

2. Average intensity for FGB in non-Kolmogorov turbulence

If we assume that a circular FGB propagates along z -axis, the optical field of the FGB at initial plane ($z=0$) can be taken in the form as [22]

$$u_0(\mathbf{r}_0, 0) = \sum_{m=1}^M (-1)^{m-1} \binom{M}{m} \exp\left(-\frac{mr_0^2}{w_0^2}\right) \exp\left(-\frac{ikr_0^2}{2R_0}\right), \quad (1)$$

where \mathbf{r}_0 is the position vector at transverse plane, w_0 is $1/e$ waist width, M is the order of FGB, $\binom{M}{m}$ denotes a binomial coefficient, R_0 is phase front radius of curvature and $k=2\pi/\lambda$ (λ is wavelength) is wave number. It should be noted that bold quantity denotes vectors, and the same quantity, which is not bold denotes its absolute value in present paper.

With the help of extended Huygens–Fresnel principle [23], the average intensity of FGB at z -plane can be expressed as

$$\langle I(\mathbf{r}, z) \rangle = \left(\frac{k}{2\pi z}\right)^2 \int_{-\infty}^{\infty} \int_{-\infty}^{\infty} \int_{-\infty}^{\infty} \int_{-\infty}^{\infty} d^2\mathbf{r}_{01} d^2\mathbf{r}_{02} u_0(\mathbf{r}_{01}) u_0^*(\mathbf{r}_{02}) MCF(\mathbf{r}_{01} - \mathbf{r}_{02}) \\ \times \exp\left\{\frac{ik}{2z} [(\mathbf{r} - \mathbf{r}_{01})^2 - (\mathbf{r} - \mathbf{r}_{02})^2]\right\} \quad (2)$$

where \mathbf{r} is radial vector at z -plane, \mathbf{r}_{01} and \mathbf{r}_{02} denote radial vectors of two different points at initial plane, respectively, and

$$MCF(\mathbf{r}_{01} - \mathbf{r}_{02}) = \langle \exp[\psi(\mathbf{r}_{01}, r) + \psi^*(\mathbf{r}_{02}, r)] \rangle = \exp[-0.5D_\psi(\mathbf{r}_{01} - \mathbf{r}_{02})] \quad (3)$$

is mutual coherence function [23,24]. In Eq.(3) D_ψ is phase structure function and approximates to D_w (wave structure function) when the effect of turbulence is not strong enough.

* Corresponding author.

E-mail address: xiuxiang_chu@yahoo.com.cn (X. Chu).

Wave structure function can be expressed by [23,25]

$$D_w(\mathbf{r}_{01}-\mathbf{r}_{02}) = 8\pi^2 k^2 \int_0^z \int_0^\infty \Phi_n(\alpha, K, z') \left[1 - J_0\left(\frac{Kz'}{z} |\mathbf{r}_{01}-\mathbf{r}_{02}| \right) \right] K dK dz' \quad (4)$$

where $J_0(x)$ is Bessel function of the first kind of order zero, K is spatial wavenumber, z is propagation distance, $\Phi_n(\alpha, K, z')$ is the 3D power spectrum of refractive index fluctuations for non-Kolmogorov turbulence and can be denoted by [5,6,8,10–13]

$$\Phi_n(\alpha, K, z') = A(\alpha) \beta(\alpha, z') K^{-\alpha} \quad (5)$$

Here, $A(\alpha) = \sin[(\alpha-3)\pi/2] \Gamma(\alpha-1)/(4\pi^2)(3 < \alpha < 5)$ is a constant that maintains consistency between index structure function and its power spectrum, $\Gamma(x)$ is Euler's gamma function, $\beta(\alpha, z')$ is general refractive index structure constant [corresponding to $C_n^2(z)$ in Kolmogorov turbulence] and has units of $m^{3-\alpha}$. If $\beta(\alpha, z')$ is independent on the propagation distance, the wave structure function can also be rewritten as [5,12]

$$D_w(\mathbf{r}_{01}-\mathbf{r}_{02}) = 2 \left(\frac{|\mathbf{r}_{01}-\mathbf{r}_{02}|}{\rho_N} \right)^{\alpha-2} \quad (3 < \alpha < 4), \quad (6)$$

where

$$\rho_N(\alpha) = \left[\frac{2^{2-\alpha} \pi^2 k^2 \alpha \beta(\alpha) z A(\alpha) \Gamma(-\alpha/2)}{(\alpha-1) \Gamma(\alpha/2)} \right]^{-1/(\alpha-2)}, \quad (7)$$

and can be interpreted as spherical wave coherence length that correspond to $\Phi_n(\alpha, K, z)$ [5]. For Kolmogorov turbulence ($\alpha=11/3$), Eq. (7) can be simplified as $\rho_N = \rho_0 = (0.545 C_n^2 k^2 z)^{-3/5}$ (spherical wave coherence length in Kolmogorov turbulence). It should be noted that Eqs. (6) and (7) are valid only when $3 < \alpha < 4$.

If $\mathbf{p} = (\mathbf{r}_{01} + \mathbf{r}_{02})/2$ and $\boldsymbol{\rho} = \mathbf{r}_{01} - \mathbf{r}_{02}$ are introduced, Eq. (2) turns out to be

$$\langle I(\mathbf{r}, \alpha) \rangle = \left(\frac{k}{2\pi z} \right)^2 \int_{-\infty}^{\infty} \int_{-\infty}^{\infty} H(\boldsymbol{\rho}) MCF(\boldsymbol{\rho}) \exp\left(\frac{ik}{z} \mathbf{r} \cdot \boldsymbol{\rho}\right) d^2 \boldsymbol{\rho} \quad (8)$$

where [23]

$$H(\boldsymbol{\rho}) = \int_{-\infty}^{\infty} \int_{-\infty}^{\infty} u_0\left(\mathbf{p} + \frac{\boldsymbol{\rho}}{2}\right) u_0^*\left(\mathbf{p} - \frac{\boldsymbol{\rho}}{2}\right) \exp\left(\frac{ik}{z} \mathbf{p} \cdot \boldsymbol{\rho}\right) d^2 \mathbf{p}. \quad (9)$$

On substituting Eq. (1) into (9), and performing the integrals we obtain

$$H(\boldsymbol{\rho}) = \sum_{m=1}^M \sum_{n=1}^M (-1)^{m+n} \binom{M}{m} \binom{M}{n} \frac{\pi w_0^2}{m+n} \times \exp\left[-\frac{(\tau_1 \tau_2 + 2im)(\tau_1 \tau_2 - 2in)}{4w_0^2(m+n)} \rho^2\right] \quad (10)$$

where $\tau_1 = 1 - z/R_0$ (beam spread factor due to geometrical magnification) and $\tau_2 = kw_0^2/z$ (Fresnel number). Inserting Eqs. (6) and (10) into (8), the average intensity can be expressed as

$$\langle I(r', \alpha) \rangle = \frac{2}{\tau_3^2} \sum_{m=1}^M \sum_{n=1}^M (-1)^{m+n} \binom{M}{m} \binom{M}{n} \frac{2}{m+n} \int_0^\infty \exp(-t^{2-\delta}) \times \exp\left[-\left(\frac{\tau^2}{\tau_3^2} - 1\right) t^2\right] J_0\left(2\sqrt{\frac{2r'}{\tau_3}} t\right) t dt, \quad (11)$$

where $t = \rho/\rho_N$, $\delta = 4 - \alpha$, $r' = r/w_0$, $\tau_3 = 2\sqrt{2}w_0/(\tau_2 \rho_N)$ (beam spread factor due to turbulence) and $\tau = \sqrt{2(\tau_1 + 2im/\tau_2)(\tau_1 - 2in/\tau_2)/(m+n) + \tau_3^2}$ (total beam spread factor). If we set $M=1$, Eq. (11) is similar to the formulae in [26,27]. Because Eq. (11) cannot be solved analytically, the average intensity with different parameters can be obtained by numerical calculation.

To obtain an analytical expression, $\exp(-t^{2-\delta})$ in Eq. (11) can be expanded in Taylor series. Namely,

$$\exp(-t^{2-\delta}) = \sum_{s=0}^{\infty} F(s) \delta^s \quad (0 < \delta < 1), \quad (12)$$

where

$$F(s) = \frac{1}{s!} \frac{d^s}{d\delta^s} \left[\exp(-t^{2-\delta}) \right]_{\delta=0}. \quad (13)$$

Therefore, Eq. (11) can be rewritten as

$$\langle I(r', \alpha) \rangle = \sum_{s=0}^{\infty} I_s(r', \alpha) \quad (14)$$

Substituting Eq. (12) into (11), the corresponding terms of the third-order Taylor series in Eq. (14) are

$$I_0(r', \alpha) = \sum_{m=1}^M \sum_{n=1}^M (-1)^{m+n} \binom{M}{m} \binom{M}{n} \frac{2}{(m+n)\tau^2} \exp\left(-\frac{2}{\tau^2} r'^2\right), \quad (15)$$

$$I_1(r', \alpha) = \sum_{m=1}^M \sum_{n=1}^M \sum_{s=0}^{\infty} (-1)^{m+n+s} \binom{M}{m} \binom{M}{n} \frac{2^{s+1} \delta r'^{2s}}{(m+n)s!^2 \tau_3^2 \tau^{2s}} A_1(2), \quad (16)$$

$$I_2(r', \alpha) = \sum_{m=1}^M \sum_{n=1}^M \sum_{s=0}^{\infty} (-1)^{m+n+s} \binom{M}{m} \binom{M}{n} \times \frac{2^{s+1} \delta^2 r'^{2s}}{(m+n)s!^2 \tau_3^2 \tau^{2s}} [A_2(3) - A_2(2)], \quad (17)$$

and

$$I_3(r', \alpha) = \sum_{m=1}^M \sum_{n=1}^M \sum_{s=0}^{\infty} (-1)^{m+n+s} \binom{M}{m} \binom{M}{n} \times \frac{2^{s+1} \delta^3 r'^{2s}}{(m+n)s!^2 \tau_3^2 \tau^{2s}} r'^{2s} [A_3(2) - 3A_3(3) + A_3(4)] \quad (18)$$

where

$$A_1(j) = \frac{1}{2} \left(\frac{\tau_3}{\tau}\right)^{2j} \Gamma(j+s) \left[\ln\left(\frac{\tau_3^2}{\tau^2}\right) + \psi(j+s) \right], \quad (19)$$

$$A_2(j) = \frac{1}{8} \left(\frac{\tau_3}{\tau}\right)^{2j} \Gamma(j+s) \left\{ \left[\ln\left(\frac{\tau_3^2}{\tau^2}\right) + \psi(j+s) \right]^2 + \psi^{(1)}(j+s) \right\}, \quad (20)$$

and

$$A_3(j) = \frac{1}{48} \left(\frac{\tau_3}{\tau}\right)^j \Gamma(s+j) \left[\ln\left(\frac{\tau_3^2}{\tau^2}\right) + \psi(s+j) \right]^3 + 3 \left[\ln\left(\frac{\tau_3^2}{\tau^2}\right) + \psi(s+j) \right] \psi^{(1)}(s+j) + \psi^{(2)}(s+j) \quad (21)$$

Here $\psi(x) = d[\ln\Gamma(x)]/dx$ is psi function, and $\psi^{(n)}(x) = d^n\psi(x)/dx^n$ is poly-gamma function. Using Eqs. (14)–(21), the average intensity of FGB in non-Kolmogorov turbulence can be calculated approximately.

3. Numerical calculation

3.1. The relative error due to the expansion in third-order Taylor series

The average intensity using the expansion in third-order Taylor series is denoted by

$$\langle I_a(r', \alpha) \rangle = \sum_{s=0}^3 I_s(r', \alpha) \quad (22)$$

and the relative error is defined as

$$\sigma = 1 - \langle I_a(r', \alpha) \rangle / \langle I(r', \alpha) \rangle. \tag{23}$$

Numerical calculation shows that the effect of M on the relative error is so small that can be ignored. The variation of on-axis relative error versus τ_3 with different δ is plotted in Fig. 1 where $\tau_1=1$ (collimated beam) and $\tau_2=20$.

It can be seen from Fig. 1 that the relative errors are small with small τ_3 , and increase with τ_3 . When we further increase τ_3 , the relative errors converge to a fixed value. Namely, if δ or τ_3 are small, Eqs. (14)–(21) provide reasonable approximations in studying the beam spreading of FGB in non-Kolmogorov turbulence.

3.2. Beam spreading of FGB in non-Kolmogorov turbulence

For non-Kolmogorov turbulence ($\alpha \neq 11/3$ or $\delta \neq 1/3$), $\beta(\alpha) \neq C_n^2$ and needs to be recalculated. Following Ref. [5], $\beta(\alpha)$ are adopted as that the power spectrum for non-Kolmogorov turbulence at a specific wavenumber is a constant. Namely, $A(\alpha)\beta(\alpha)K_m^{-\alpha} = A(11/3)C_n^2K_m^{-11/3}$. Therefore, $\beta(\alpha)$ can be written as

$$\beta(\alpha) = \frac{A(11/3)}{A(\alpha)} C_n^2 K_m^{\alpha-11/3}, \tag{24}$$

where K_m is chosen as $K_m \approx (k/z)^{1/2}$ [13]. The normalized average intensity is defined as

$$\langle I_n(r', \alpha) \rangle = \frac{\langle I_a(r', \alpha) \rangle}{\langle I_a(0, 11/3) \rangle} \tag{25}$$

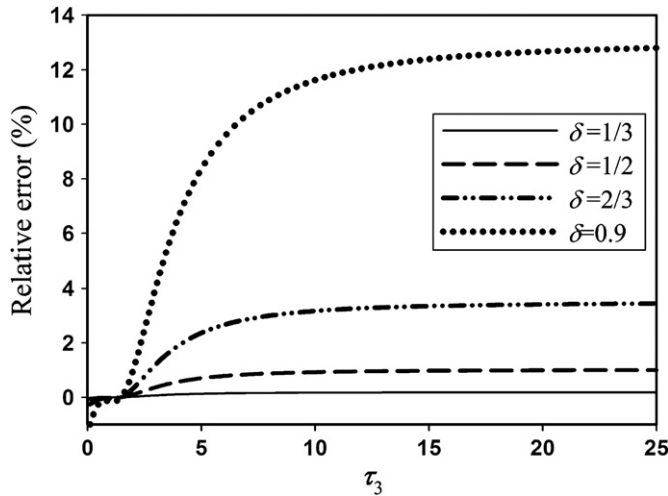


Fig. 1. Variation of relative error with different δ and τ_3 where $M=5$, $\tau_1=1$ and $\tau_2=20$.

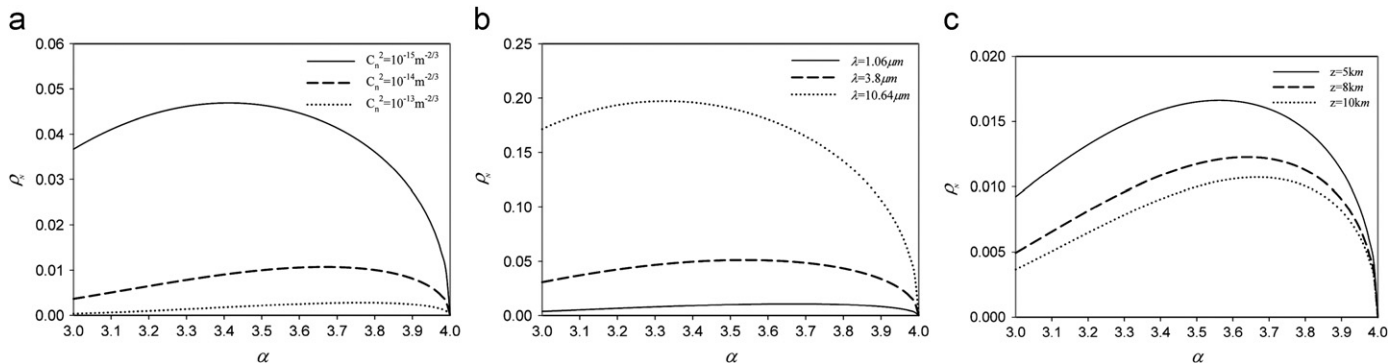


Fig. 2. Variation of ρ_N with α (a) $\lambda=1.06 \mu\text{m}$ and $z=10 \text{ km}$; (b) $C_n^2 = 10^{-14} \text{ m}^{-2/3}$ and $z=10 \text{ km}$; (c) $C_n^2 = 10^{-14} \text{ m}^{-2/3}$ and $\lambda=1.06 \mu\text{m}$.

Because τ_3 is inversely proportional to ρ_N when Fresnel number τ_2 and w_0 are constants, the variations of ρ_N with different parameters are plotted in Fig. 2.

Fig. 2 shows that ρ_N increases with α when α is small. With the increase in α , ρ_N gradually reaches a maximum value and then decrease. When α approaches 4, ρ_N approaches zero. This can be explained that $\alpha=4$ implies tilt only [28] and results in a wide spot with a very low irradiance peak [29]. When C_n^2 is larger or λ is shorter, the variation of ρ_N with α is smaller.

Substituting Eq. (24) into (7), we also obtain

$$\rho_N = \left[\frac{2.39 \times 2^{-\alpha} \alpha \Gamma(-\alpha/2)}{(\alpha-1)\Gamma(\alpha/2)} \right]^{-1/(\alpha-2)} \tau_2^{(11-3\alpha)/(6(\alpha-2))} \left(\frac{w_0}{\rho_0} \right)^{(3\alpha-11)/(3(\alpha-2))} \rho_0. \tag{26}$$

From Eqs. (11) and (26) we can see that the average intensity distribution of FGB in non-Kolmogorov turbulence is determined by M , τ_1 , τ_2 , α , w_0 and ρ_0 . For convenience, we set $\tau_1=1$ ($R_0 \rightarrow \infty$) in the following calculation. The intensity profiles of FGB against ρ_0 with different α are shown in Fig. 3 where $\tau_2=10$, $w_0=0.3 \text{ m}$ and $M=5$.

It shows that the effect of turbulence on the intensity profiles is smaller for $\alpha=11/3$ than that for $\alpha=7/2$ and $10/3$. When $\rho_0=0.2 \text{ m}$, the intensity profiles still remain flat shapes. With the decrease of ρ_0 , the intensity profiles gradually become the shape of Gaussian distribution. The intensity for $\alpha=10/3$ spread faster than that for $\alpha=11/3$ and $7/2$. The variation of on-axis normalized intensity with ρ_0 is plotted in Fig. 4.

It can be seen from Fig. 4 that when ρ_0 is small, the on-axis normalized intensity is small and independent on M . With the increase of ρ_0 , the on-axis normalized intensity increase and the difference with different M become large. The on-axis normalized intensity is larger for smaller M . From Fig. 4 we also can see that the on-axis normalized intensity is smaller for $\alpha=10/3$ than that for $\alpha=7/2$ when ρ_0 is small.

The variations of the on-axis normalized intensity versus Fresnel number are plotted in Fig. 5. It shows that when Fresnel number is small (in far field), the on-axis normalized intensity is small and independent on M . With the increase in Fresnel number, the on-axis normalized intensity increase. When Fresnel number is large enough (in near field), the on-axis normalized intensity is different with different M . Comparing Fig. 5a with b we also can see that the on-axis normalized intensity for $\alpha=7/2$ is larger than that for $\alpha=10/3$.

The effects of waist width on the on-axis normalized intensity are shown in Fig. 6. It illustrates that the variation of the on-axis normalized intensity due to M is small when w_0 is large or small. When w_0 is very small the on-axis normalized intensity is 1 for any M and α . With the increase of w_0 the on-axis normalized intensity increase and gradually reaches its maximum value. As the waist width w_0 further increase the on-axis normalized

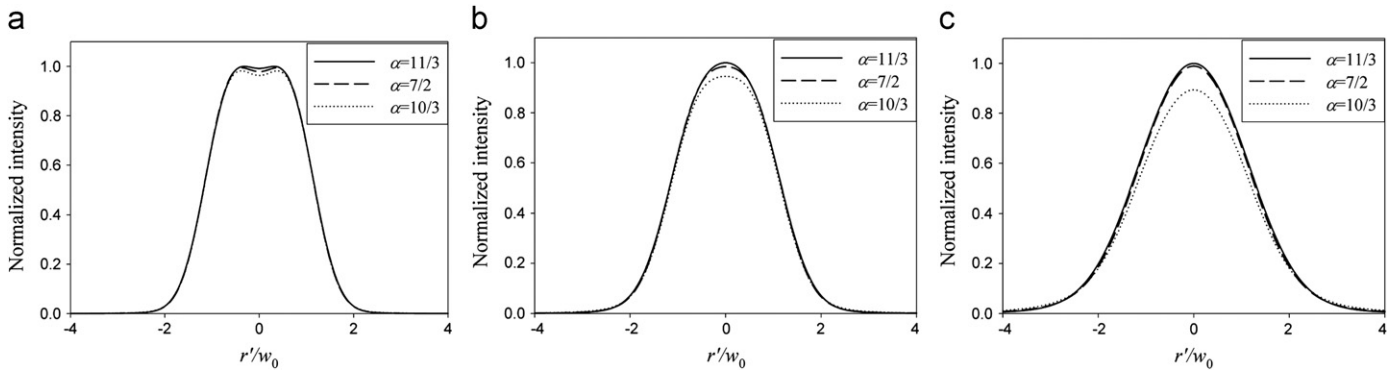


Fig. 3. Intensity profiles of FGB with different α where $\tau_2=10$, $w_0=0.3$ m and $M=5$; (a) $\rho_0=0.2$ m; (b) $\rho_0=0.1$ m; (c) $\rho_0=0.05$ m.

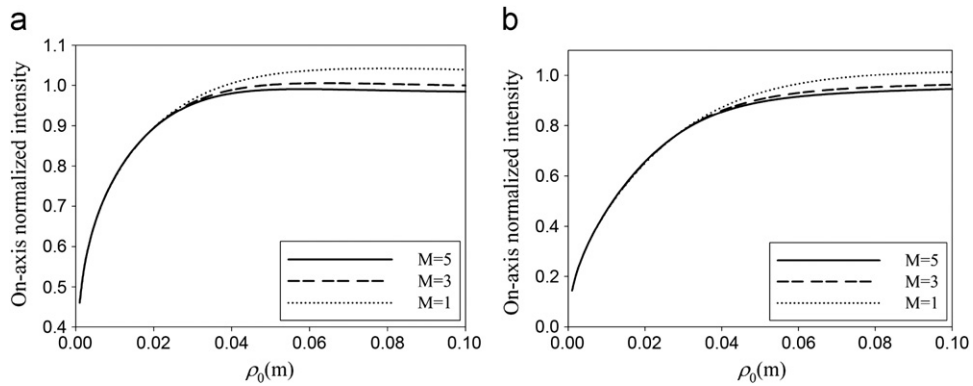


Fig. 4. Variation of on-axis normalized intensity with ρ_0 where $\tau_2=10$ and $w_0=0.3$ m; (a) $\alpha=7/2$; (b) $\alpha=10/3$.

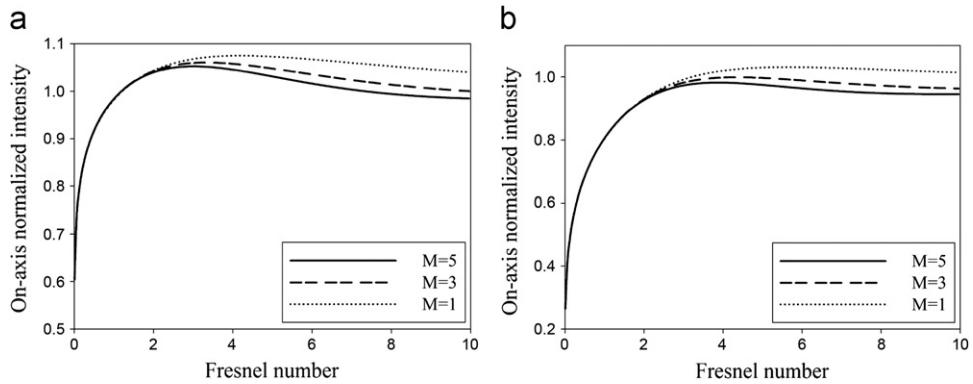


Fig. 5. Variation of on-axis normalized intensity with τ_2 where $\rho_0=0.1$ m, $w_0=0.3$ m; (a) $\alpha=7/2$; (b) $\alpha=10/3$.

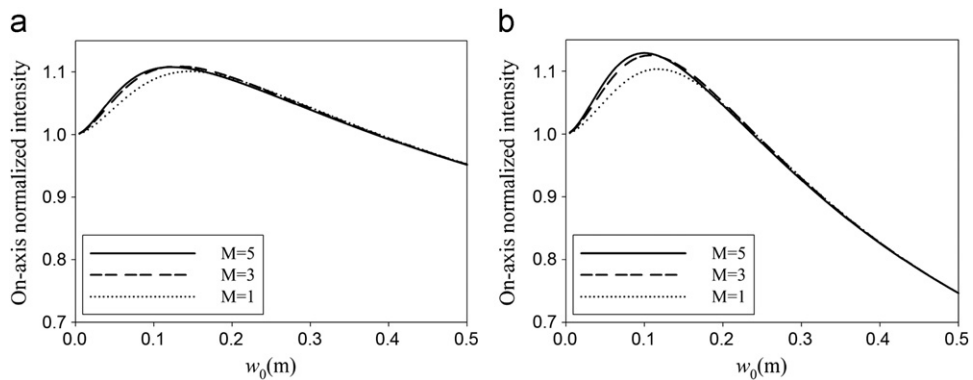


Fig. 6. Variation of on-axis normalized intensity with w_0 where $\rho_0=0.1$ m, $\tau_2=2$; (a) $\alpha=7/2$; (b) $\alpha=10/3$.

intensity becomes smaller and smaller. The change of the on-axis normalized intensity is smaller for $\alpha=7/2$ than that for $\alpha=10/3$ by comparing Fig. 6a with b.

4. Conclusion

Based on the extended Huygens–Fresnel principle, the analytical expression for average intensity of FGB in non-Kolmogorov turbulence is obtained using expansion in third-order Taylor series. Numerical calculation shows that the third-order expression should provide reasonable approximations if δ or τ_3 is small. In addition, more higher-order expression could be derived easily with the same way.

From the studies we can see that the average intensity is determined only by M , τ_1 , τ_2 , α , w_0 and ρ_0 . When Fresnel number τ_2 or coherence length ρ_0 is small, or w_0 is very large or very small, the effects of M on the normalized average intensity is so small that can be neglected. However, the average intensity is obvious difference with different α . It should be noted that the analysis is based on the assumption of Eq. (24). Results are different with different relation between $\beta(\alpha)$ and C_n^2 .

Acknowledgment

The project was supported by Open Research Fund of the Key Laboratory of Atmospheric Composition and Optical Radiation, Chinese Academy of Sciences (JJ0903).

References

- [1] Buser RG. Interferometric determination of the distance dependence of the phase structure for near-ground horizontal propagation at 6328 angstroms. *J Opt Soc Am* 1971;61:488–91.
- [2] Dayton D, Pierson B, Spielbusch B, Gonglewski J. Atmospheric structure function measurement with a Shack-Hartmann wavefront sensor. *Opt Lett* 1992;17:1737–9.
- [3] Golbraikh E, Moiseev SS. Different spectra formation in the presence of helical transfer. *Phys Lett A* 2002;305:173–5.
- [4] Rao C, Jiang W, Ling N. Spatial and temporal characterization of phase fluctuations in non-Kolmogorov atmospheric turbulence. *J Mod Opt* 2000;47:1111–1126.
- [5] Stribling BE, Welsh BM, Roggemann MC. Optical propagation in non-Kolmogorov atmospheric turbulence. *Proc SPIE* 1995;2471:181–96.
- [6] Boreman GD, Dainty C. Zernike expansions for non-Kolmogorov turbulence. *J Opt Soc Am A* 1996;13:517–22.
- [7] Rao C, Jiang W, Ling N. Adaptive-optics compensation by distributed beacons for non-Kolmogorov turbulence. *Appl Opt* 2001;40:3441–9.
- [8] Golbraikh E, Kopeika NS. Behavior of structure function of refraction coefficients in different turbulent fields. *Appl Opt* 2004;43:6151–6.
- [9] Golbraikh E, Branover H, Kopeika NS, Zilberman A. Non-Kolmogorov atmospheric turbulence and optical signal propagation. *Nonlinear Processes Geoph* 2006;13:297–301.
- [10] Toselli I, Andrews LC, Phillips RL, Ferrero V. Angle of arrival fluctuations for free space laser beam propagation through non Kolmogorov turbulence. *Proc SPIE* 2007;65510E:1–12.
- [11] Toselli I, Andrews LC, Phillips RL, Ferrero V. Free-space optical system performance for laser beam propagation through non-Kolmogorov turbulence. *Opt Eng* 2008;47:026003-1–9.
- [12] Pérez DG, Zunino L. Generalized wavefront phase for non-Kolmogorov turbulence. *Opt Lett* 2008;33:572–4.
- [13] Zilberman A, Golbraikh E, Kopeika NS. Propagation of electromagnetic waves in Kolmogorov and non-Kolmogorov atmospheric turbulence: three-layer altitude model. *Appl Opt* 2008;47:6385–91.
- [14] Kopeika NS, Zilberman A, Golbraikh E. Imaging and communications through non-Kolmogorov turbulence. *Proc SPIE* 2009;7463:746307-1–12.
- [15] Eyyuboğlu HT, Baykal Y. Reciprocity of cos-Gaussian and cosh-Gaussian laser beams in turbulent atmosphere. *Opt Express* 2004;12:4659–74.
- [16] Cai Y, He S. Propagation of various dark hollow beams in turbulent atmosphere. *Opt Exp* 2006;14:1353–67.
- [17] Eyyuboğlu HT, Arpali C, Baykal Y. Flat topped beams and their characteristics in turbulent media. *Opt Express* 2006;14:4196–207.
- [18] Chu X, Ni Y, Zhou G. Propagation analysis of flattened circular Gaussian beams with a circular aperture in turbulent atmosphere. *Opt Commun* 2007;274:274–280.
- [19] Chu X. Propagation of a cosh-Gaussian beam through an optical system in turbulent atmosphere. *Opt Express* 2007;24:17613–8.
- [20] Chu X, Liu Z, Wu Y. Propagation of a general multi-Gaussian beam in turbulent atmosphere in a slant path. *J Opt Soc Am A* 2008;25:74–9.
- [21] Zhu Y, Zhao D, Du X. Propagation of stochastic Gaussian-Schell model array beams in turbulent atmosphere. *Opt Express* 2008;16:18437–42.
- [22] Li Y. Light beams with flat-topped profiles. *Opt Lett* 2002;27:1007–9.
- [23] Yura HT, Hanson SG. Optical beam wave propagation through complex optical system. *J Opt Soc Am A* 1987;4:1931–48.
- [24] Wang SCH, Plonus MA. Optical beam propagation for a partially coherent source in the turbulent atmosphere. *J Opt Soc Am* 1979;69:1297–304.
- [25] Clifford SF. The classical theory of wave propagation in a turbulent medium. In: Strohbehn J, editor. *Laser beam propagation in the atmosphere*. Springer; 1978.
- [26] Gochelashvily KS, Shishov VI. Focused irradiance fluctuations beyond a layer of turbulent atmosphere. *Opt Acta* 1972;19:327–32.
- [27] Gochelashvily KS. Focused laser irradiance fluctuations in a turbulent medium. *Opt Acta* 1973;20:193–206.
- [28] Wandzura SM. Meaning of quadratic structure functions. *J Opt Soc Am* 1980;70:745.
- [29] Stribling BE. *Laser beam propagation in non-Kolmogorov atmospheric turbulence*. MS thesis, Air Force Institute of Technology, Wright-Patterson Air Force Base, Ohio, 1994.